

可視光赤外線観測の現状 ~アウトフローの観測~

Recent Results of Outflow Observations

国立天文台 水沢VLBI観測所 石垣島天文台

特任研究員 堀内 貴史

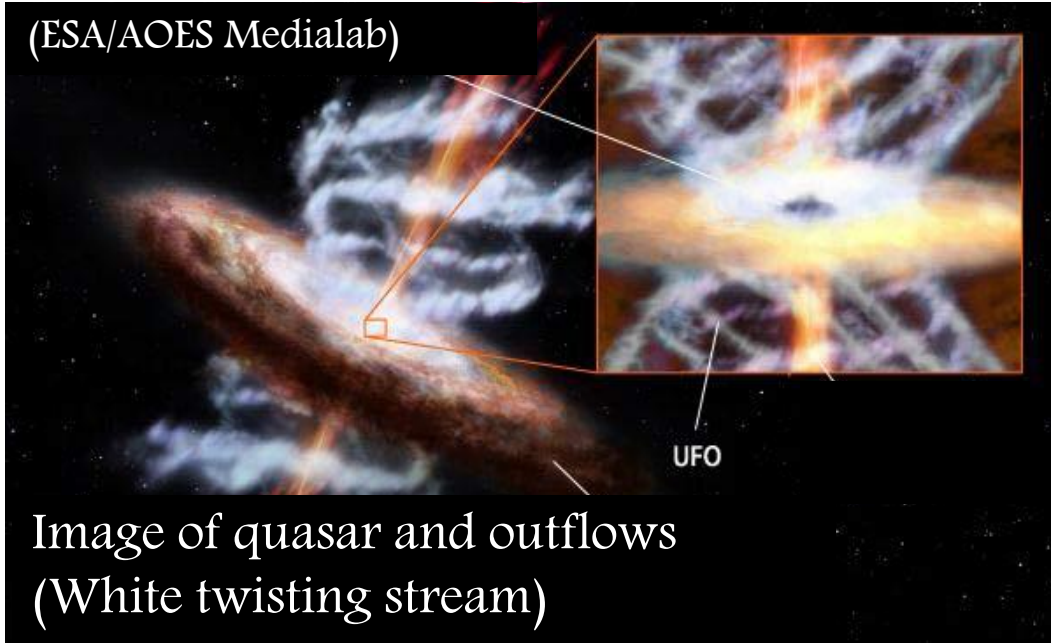
Takashi Horiuchi (NAOJ)

Contents

- Observational evidence of quasar outflows – BALs, mini-BALs, NALs –
- BAL to non-BAL quasar transformations !? (Sameer et al. 2018, arXiv:1810.03625v2)
- BAL quasar at a redshift of 7.02 ! (Wang et al. 2018, arXiv:1810.11925)

Quasar Outflows

(ESA/AOES Medialab)



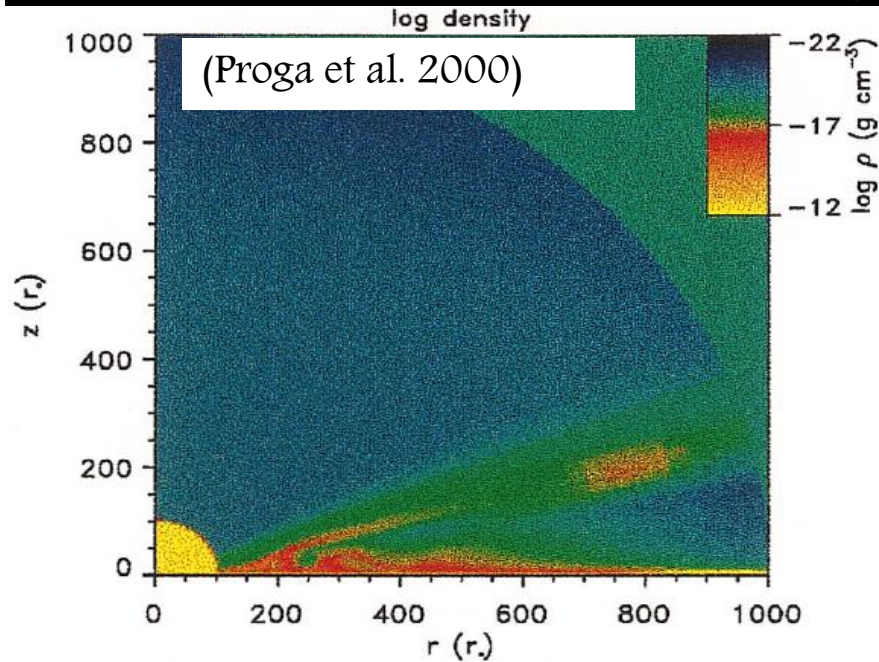
Quasar outflows are important element for

- (i) quasar growth,
- (ii) chemical evolution for host galaxy and intergalactic space

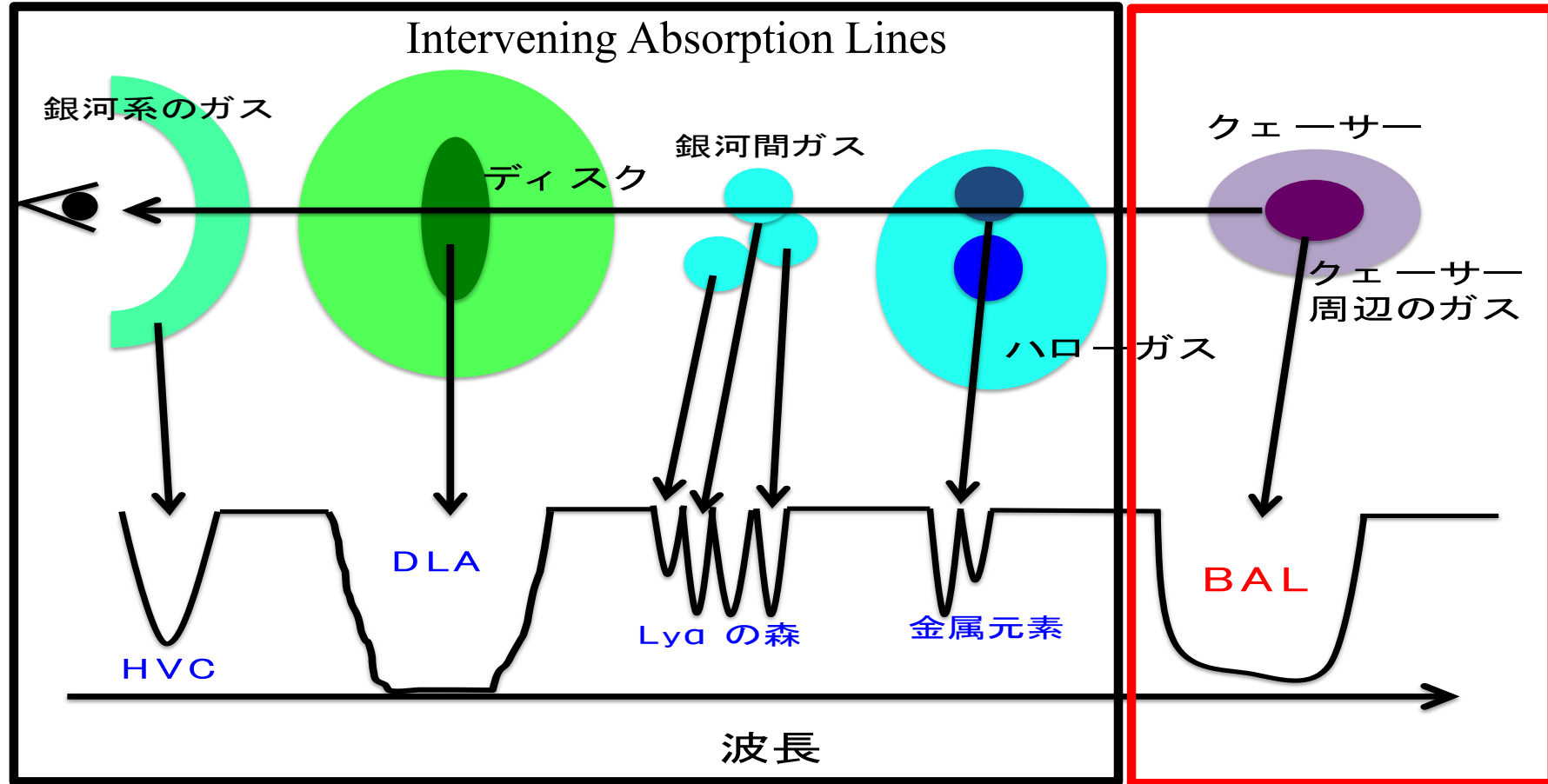
Mechanisms to launch outflows (candidates)

- Radiation pressure (Proga et al. 2000; Nomura et al. 2012, 2015)
- Magnetic Force (Everett 2005)

Using quasar absorption lines to study outflows !



Quasar Absorption Line

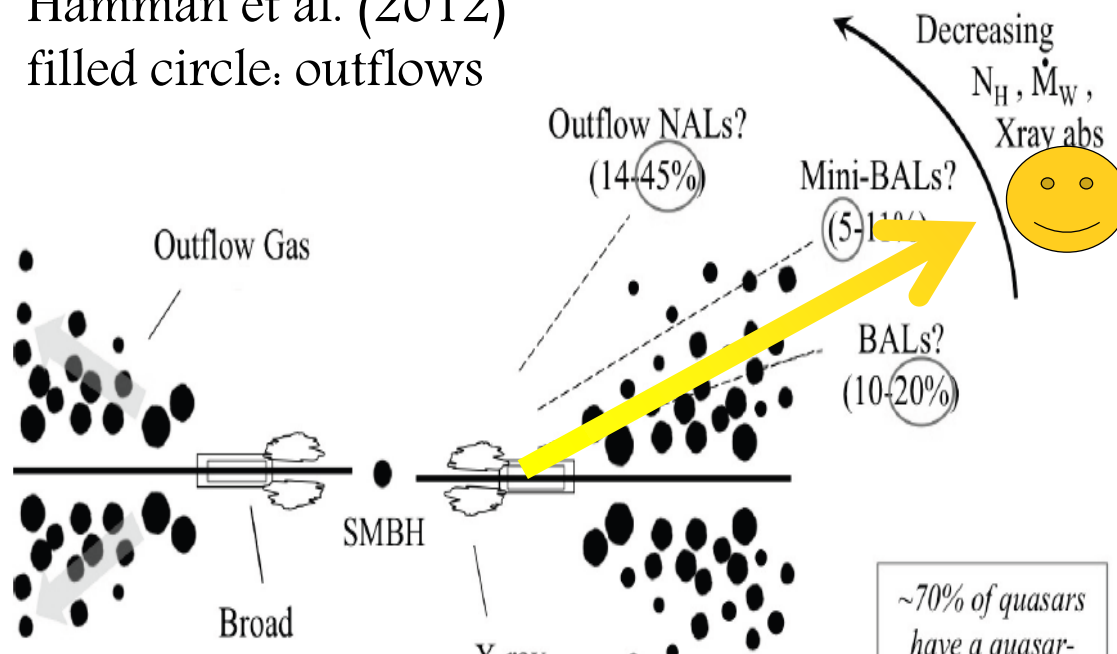


- Intervening Absorption Lines: IGM , CGM etc
- Intrinsic Absorption Lines : Outflow Gas

Intrinsic Absorption
Lines

Quasar intrinsic absorption lines: BALs, mini-BALs and NALs

Hamman et al. (2012)
filled circle: outflows

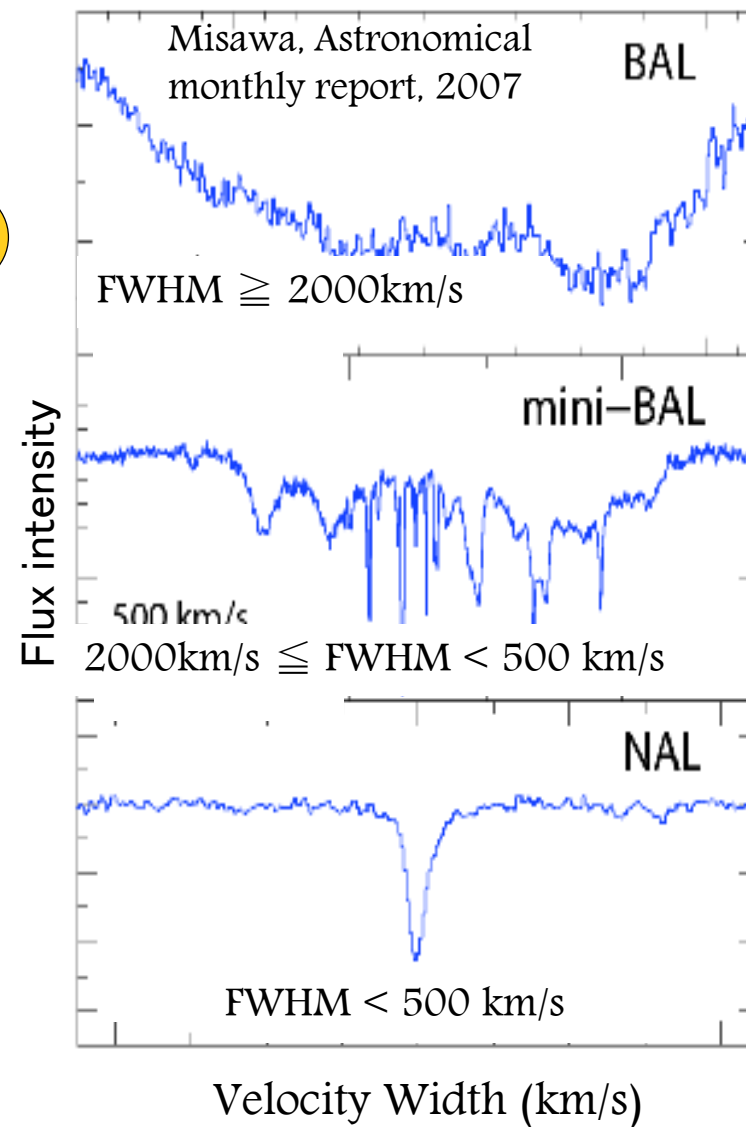


BALs: The main current of outflow study

mini-BALs and NALs: They are attracting attention in recent year

Estimation of physical parameters is possible !

AL via outflows



About Broad Absorption Lines (BALs)

- Definition for BALs: Balnicity Index (Weymann et al. 1991)

$$\text{BI} = \int_{v_{\min}}^{v_{\max}} \left(1 - \frac{f(v)}{0.9} \right) C dv$$

normalized spectrum

1 : Quantity in brackets is continuously greater than zero for more than 2,000 km/s
0: otherwise

- Velocities are usually set to 3,000 and 25,000 km/s

To avoid strong absorption complexes around blueward of C IV emission

To avoid ambiguities with Si IV emission and absorption

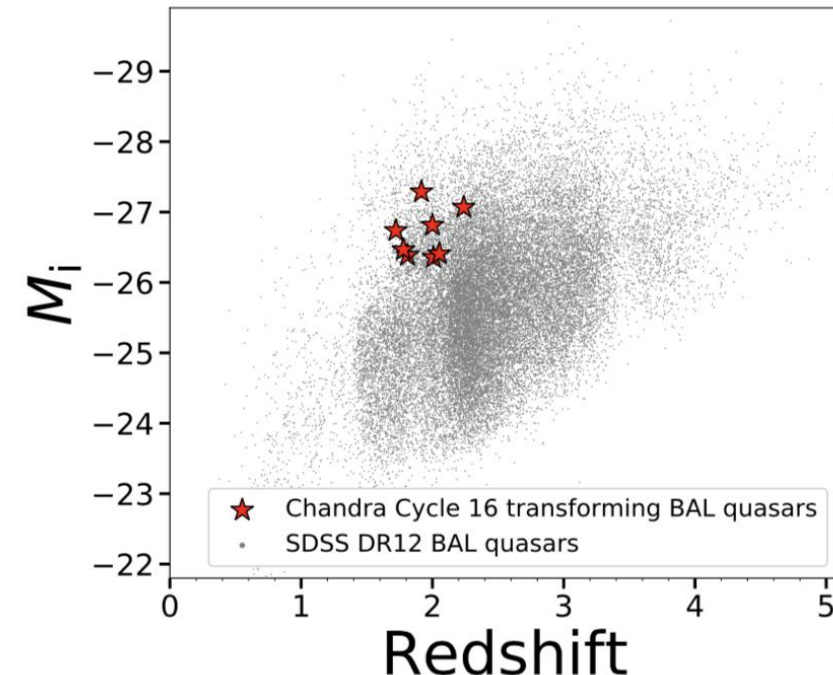
- BI(maximum) = 20,000 km/s (=25,000-3,000-2,000) km/s

Contents

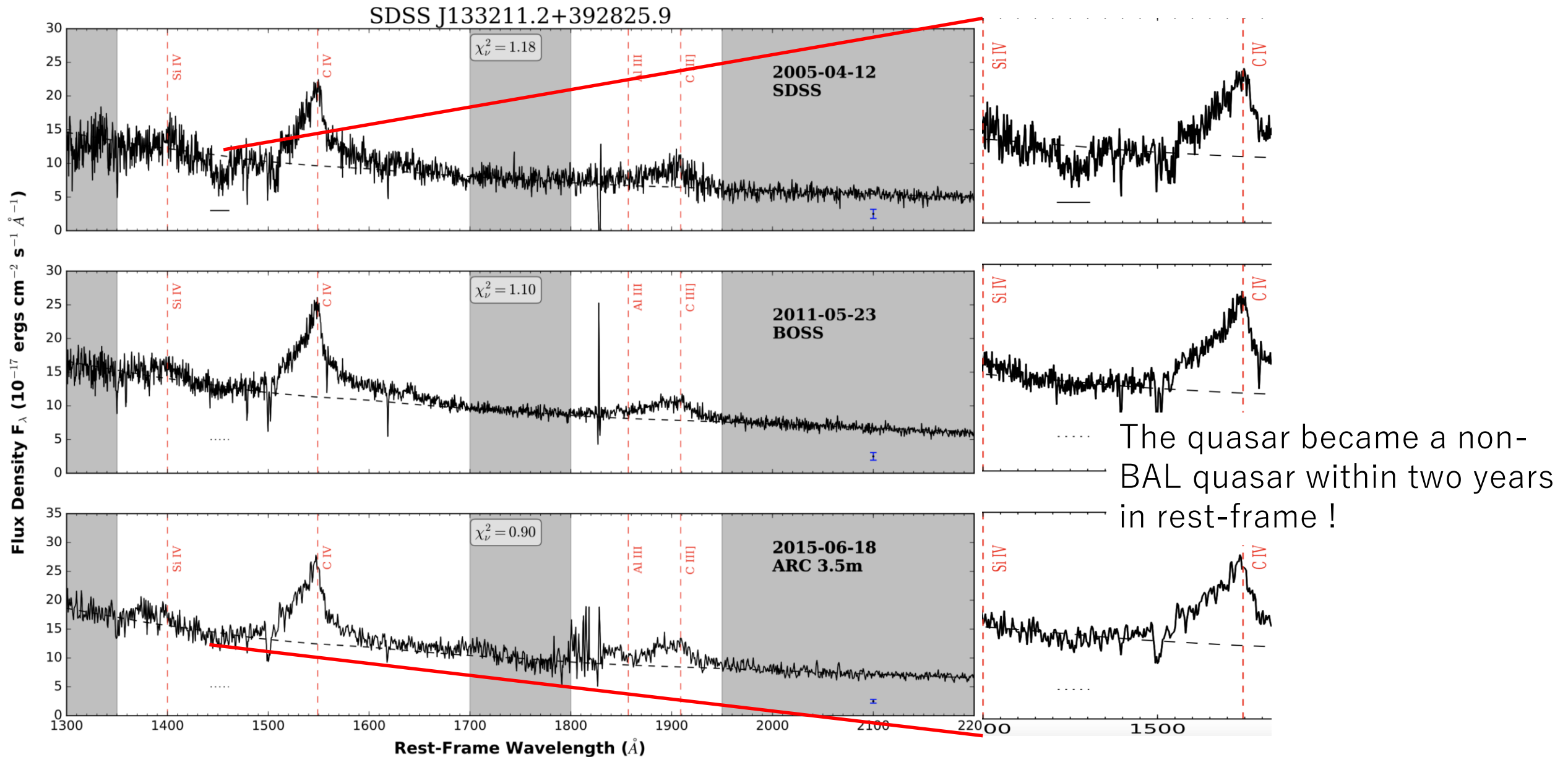
- Observational evidence of quasar outflows – BALs, mini-BALs, NALs –
- BAL to non-BAL quasar transformations !? (Sameer et al. 2018, arXiv:1810.03625v2)
- BAL quasar at a redshift of 7.02 ! (Wang et al. 2018, arXiv:1810.11925)

Samerr et al. (2018) : ABSTRACT

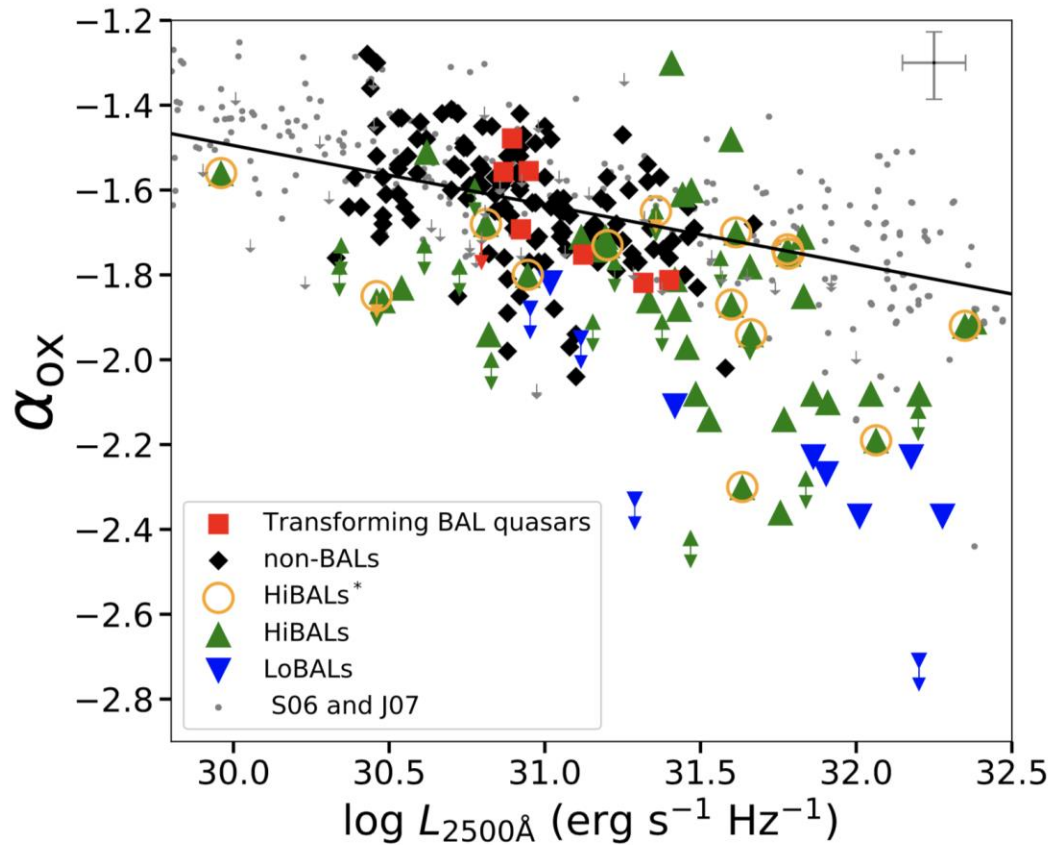
- Theme: X-ray and optical/UV study of eight BAL to non-BAL transforming quasars at $z \approx 1.7\text{--}2.2$ over 0.29–4.95 rest-frame years.
- Data:
SDSS, BOSS, Gemini, and ARC 3.5-m (optical), Chandra (X-ray)
- Results:
New Chandra observations show α_{OX} and $\Delta\alpha_{\text{OX}}$ of are consistent with those
- Conclusion: X-ray and optical/UV observation
 - (At least) The X-ray absorbing material moving out of the line-of-sight, leaving an X-ray unabsorbed non-BAL quasar.
 - The UV absorber might have become more highly ionized (in a shielding-gas scenario) or also moved out of the line-of-sight (in a wind-clumping scenario).



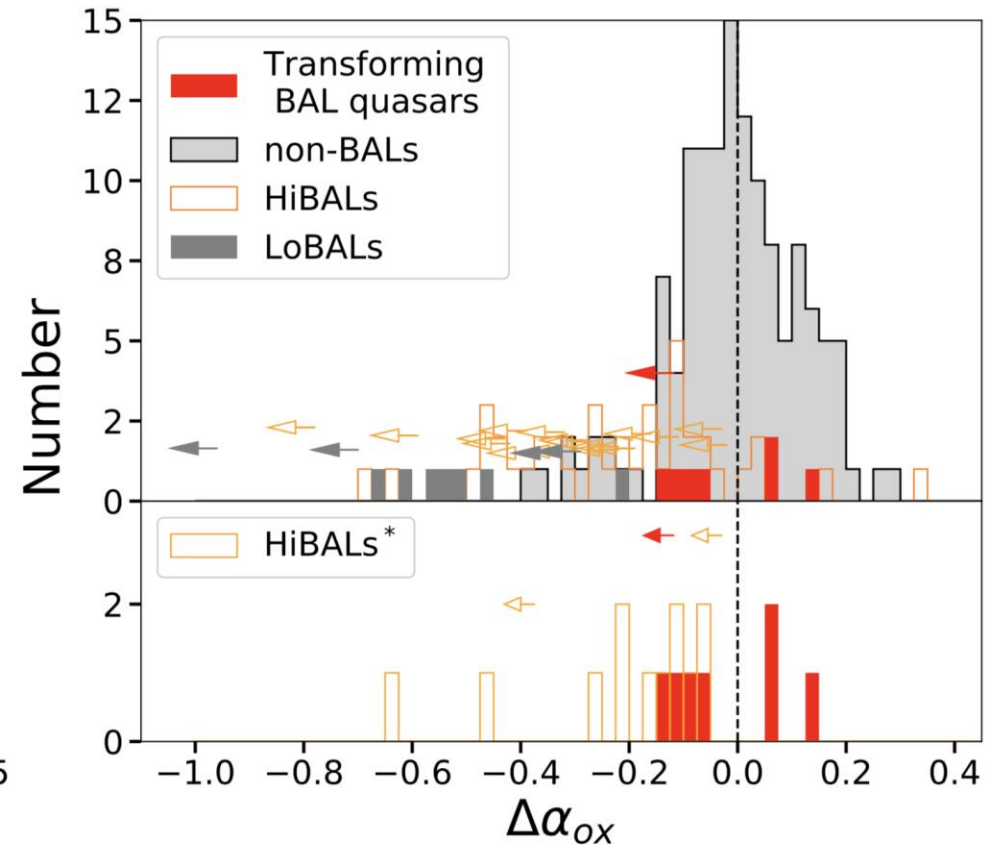
An Example of non-BAL transforming



Comparing X-ray-to-optical power-law slope α_{ox} and $\Delta\alpha_{\text{ox}}$



$$\alpha_{\text{ox}} = \frac{\log(f_{2\text{ keV}}/f_{2500\text{ \AA}})}{\log(\nu_{2\text{ keV}}/\nu_{2500\text{ \AA}})}$$



$$\Delta\alpha_{\text{ox}} = \alpha_{\text{ox}(\text{measured})} - \alpha_{\text{ox}(\text{expected})}$$

$$\alpha_{\text{ox}(\text{expected})} = (-0.140 \pm 0.007) \log(L_{2500\text{ \AA}}) + (2.705 \pm 0.212)$$

X-ray, optical, and radio properties

| Object Name (SDSS J) | z | m_i | M_i | N_H | Count Rate | $F_{0.5-2 \text{ keV}}$ | $f_2 \text{ keV}$ | $\log L_X$ (2–10 keV) | $f_{2500 \text{ \AA}}$ | $\log L_\nu$ (2500 \AA) | α_{ox} | $\Delta\alpha_{ox}(\sigma)$ | R |
|----------------------|------|-------|--------|-------|------------------------|-------------------------|-------------------------|--------------------------|------------------------|--------------------------------------|-------------------------|-----------------------------|-------|
| (1) | (2) | (3) | (4) | (5) | (6) | (7) | (8) | (9) | (10) | (11) | (12) | (13) | (14) |
| 074650.59+182028.7 | 1.92 | 17.96 | −27.36 | 4.17 | $1.63^{+1.27}_{-0.77}$ | $0.94^{+0.79}_{-0.53}$ | $4.11^{+3.43}_{-2.30}$ | 44.46 | 2.24 ± 0.22 | 31.32 ± 0.10 | $-1.82^{+0.10}_{-0.08}$ | −0.14(0.89) | <2.17 |
| 085904.59+042647.8 | 1.81 | 18.74 | −26.45 | 4.11 | < 1.0 | <0.57 | <2.39 | <44.18 | 0.75 ± 0.07 | 30.80 ± 0.10 | <−1.72 | <−0.12(0.64) | <4.46 |
| 093620.52+004649.2 | 1.72 | 18.26 | −26.81 | 3.85 | $4.38^{+1.72}_{-1.28}$ | $2.51^{+1.24}_{-1.05}$ | $10.21^{+5.05}_{-4.27}$ | 44.77 | 1.15 ± 0.12 | 30.95 ± 0.10 | $-1.56^{+0.07}_{-0.06}$ | 0.07(0.41) | <2.94 |
| 114546.22+032251.9 | 2.01 | 19.01 | −26.42 | 2.19 | $2.54^{+0.95}_{-0.71}$ | $1.40^{+0.67}_{-0.58}$ | $6.31^{+3.02}_{-2.58}$ | 44.68 | 0.72 ± 0.07 | 30.87 ± 0.10 | $-1.56^{+0.07}_{-0.06}$ | 0.06(0.33) | <5.74 |
| 133211.21+392825.9 | 2.05 | 19.01 | −26.46 | 0.89 | $4.31^{+1.17}_{-0.94}$ | $2.31^{+0.93}_{-0.86}$ | $10.49^{+4.24}_{-3.89}$ | 44.91 | 0.75 ± 0.08 | 30.89 ± 0.10 | $-1.48^{+0.06}_{-0.06}$ | 0.14(0.79) | <5.21 |
| 142132.01+375230.3 | 1.78 | 18.61 | −26.54 | 0.92 | $1.79^{+1.05}_{-0.70}$ | $0.96^{+0.63}_{-0.47}$ | $3.99^{+2.63}_{-1.96}$ | 44.38 | 1.02 ± 0.10 | 30.92 ± 0.10 | $-1.69^{+0.09}_{-0.07}$ | −0.07(0.38) | <3.66 |
| 152149.78+010236.4 | 2.24 | 18.45 | −27.22 | 4.24 | $1.39^{+0.92}_{-0.59}$ | $0.81^{+0.59}_{-0.42}$ | $3.89^{+2.83}_{-2.02}$ | 44.55 | 2.04 ± 0.21 | 31.40 ± 0.10 | $-1.81^{+0.09}_{-0.07}$ | −0.12(0.79) | <3.96 |
| 152243.98+032719.8 | 2.00 | 18.56 | −26.86 | 3.81 | $1.39^{+0.92}_{-0.59}$ | $0.80^{+0.58}_{-0.41}$ | $3.57^{+2.60}_{-1.86}$ | 44.43 | 1.31 ± 0.13 | 31.12 ± 0.10 | $-1.75^{+0.09}_{-0.07}$ | −0.10(0.59) | <3.88 |

New Chandra Observation

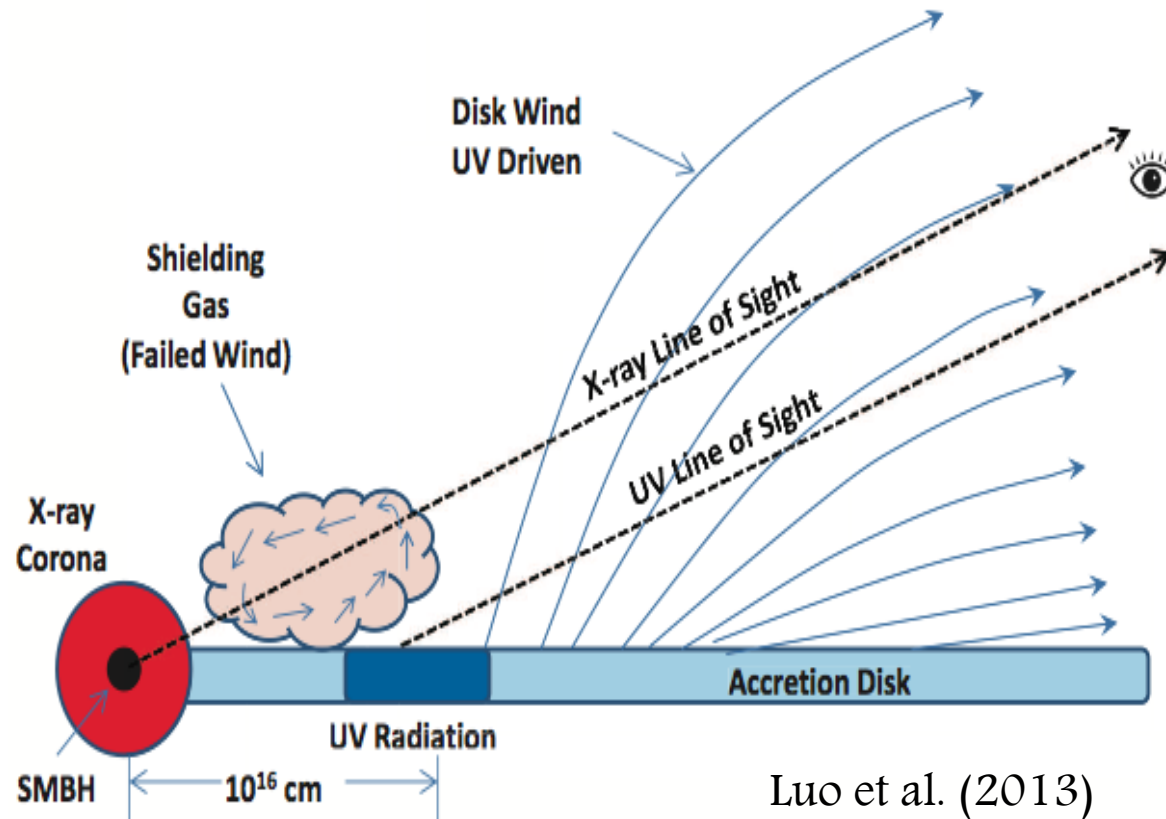
Table 3. *Chandra* observation log and X-ray counts

| Object Name (SDSS J) | ObsID | Date | Exposure Time (ks) | Full-Band Cts. (0.5–8.0 keV) | Soft-Band Cts. (0.5–2.0 keV) | Hard-Band Cts. (2.0–8.0 keV) | Band Ratio | Γ_{eff} |
|----------------------|-------|-------------|-----------------------|---------------------------------|---------------------------------|---------------------------------|------------------------|------------------------|
| (1) | (2) | (3) | (4) | (5) | (6) | (7) | (8) | (9) |
| 074650.59+182028.7 | 17021 | 2015 Dec 03 | 2.54 | $9.51^{+4.21}_{-3.04}$ | $4.15^{+3.22}_{-1.95}$ | $5.46^{+3.50}_{-2.27}$ | $1.32^{+1.02}_{-0.69}$ | $0.67^{+0.72}_{-0.54}$ |
| 085904.59+042647.8 | 17023 | 2016 Jan 04 | 3.92 | $3.09^{+2.99}_{-1.69}$ | < 4.07 | $2.13^{+2.72}_{-1.36}$ | > 0.52 | < 1.56 |
| 093620.52+004649.2 | 17022 | 2015 Mar 16 | 2.61 | $13.76^{+4.82}_{-3.67}$ | $11.44^{+4.50}_{-3.33}$ | $2.15^{+2.72}_{-1.36}$ | $0.19^{+0.24}_{-0.13}$ | $2.55^{+1.06}_{-0.80}$ |
| 114546.22+032251.9 | 17029 | 2016 Feb 09 | 4.91 | $16.88^{+5.22}_{-4.08}$ | $12.46^{+4.64}_{-3.49}$ | $4.30^{+3.27}_{-2.01}$ | $0.34^{+0.28}_{-0.18}$ | $1.93^{+0.70}_{-0.57}$ |
| 133211.21+392825.9 | 17028 | 2015 Aug 24 | 4.83 | $25.48^{+6.13}_{-5.02}$ | $20.84^{+5.65}_{-4.53}$ | $4.35^{+3.27}_{-2.01}$ | $0.21^{+0.16}_{-0.10}$ | $2.38^{+0.64}_{-0.55}$ |
| 142132.01+375230.3 | 17027 | 2015 Oct 07 | 3.49 | $7.38^{+3.86}_{-2.66}$ | $6.24^{+3.65}_{-2.43}$ | < 4.26 | < 0.68 | > 1.25 |
| 152149.78+010236.4 | 17026 | 2015 Jun 12 | 3.73 | $6.29^{+3.67}_{-2.46}$ | $5.18^{+3.44}_{-2.20}$ | < 4.23 | < 0.82 | > 1.13 |
| 152243.98+032719.8 | 17024 | 2015 Apr 12 | 3.73 | $11.62^{+4.53}_{-3.37}$ | $5.18^{+3.44}_{-2.20}$ | $6.56^{+3.71}_{-2.50}$ | $1.27^{+0.88}_{-0.61}$ | $0.70^{+0.64}_{-0.50}$ |

Column (1): The SDSS J2000 equatorial coordinates for the quasar. Column (2): *Chandra* observation ID. Column (3): Date of observation of the target with *Chandra*. Column (4): Background-flare cleaned effective exposure time. Columns (5), (6), (7): The X-ray data analysis was carried out using the procedure in [Luo et al. \(2015\)](#). Errors on the X-ray counts were calculated using Poisson statistics corresponding to the 1σ significance level using [Gehrels \(1986\)](#). A source is considered undetected if the P_{B} value, defined via Equation (3) in Section 3.1, in a band is > 0.01, in which case an upper limit on the source counts was derived. Column (8): Band ratio is the hard band to soft band ratio. Column (9): The effective power-law photon index, Γ_{eff} .

Consideration about ancillary mechanism

Are ionization states in outflows influenced by changing optical thickness of X-ray shielding gas observed by X-ray !?



Luo et al. (2013)

Eight transforming BAL quasars show no evidence for intrinsic X-ray absorption

→ X-ray absorbing material moving out of the line-of-sight !

Generally, BAL quasars show strong intrinsic X-ray absorption

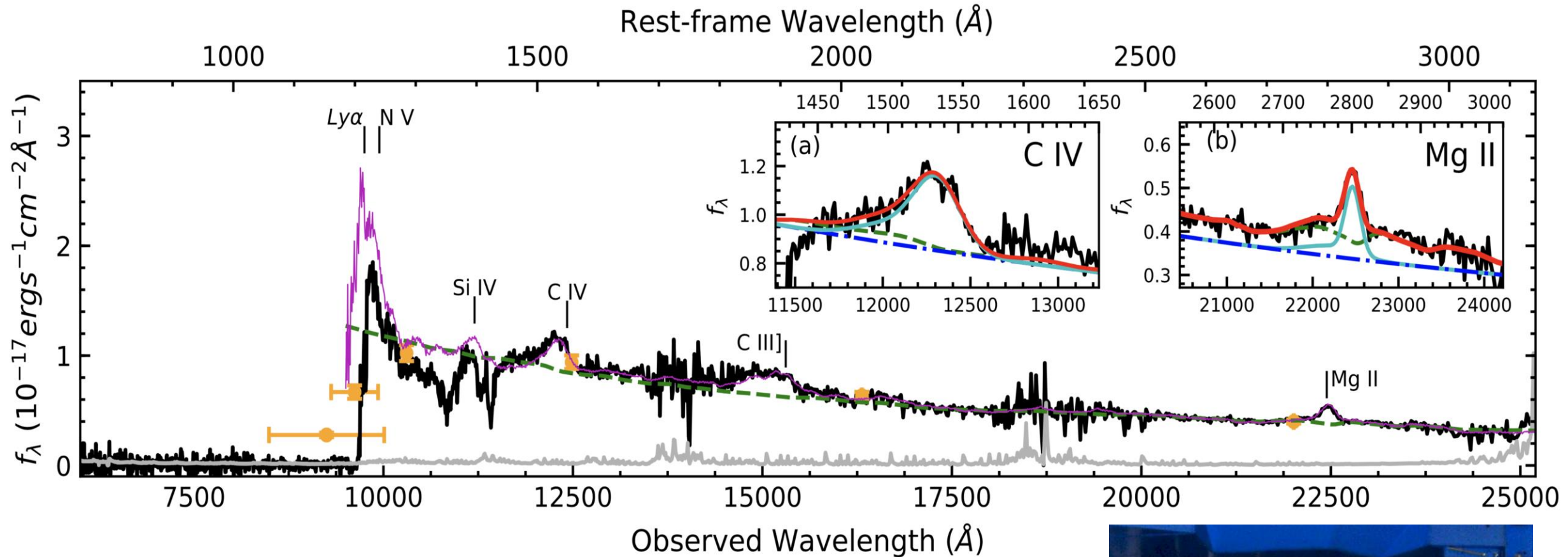
Contents

- Observational evidence of quasar outflows – BALs, mini-BALs, NALs –
- BAL to non-BAL quasar transformations !? (Sameer et al. 2018, arXiv:1810.03625v2)
- BAL quasar at a redshift of 7.02 (Wang et al. 2018, arXiv:1810.11925)

Wang et al. (2018) : ABSTRACT

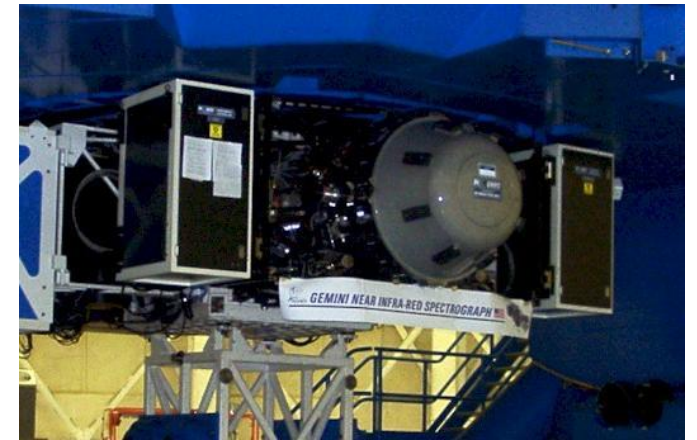
- Theme: The discovery of a luminous quasar at $z = 7.021$, DELS J003836.10– 152723.6 (hereafter J0038–1527), selected using photometric data.
- Photometric data :
DESI Legacy imaging Survey (DELS), Pan-STARRS1 (PS1) imaging Survey,
WISE mid-infrared all-sky survey
- J0038–1527 is the most luminous quasar known at $z > 7$ ($L_{\text{Bol}} = 5.6 \times 10^{13} L_{\odot}$)
 - ✧ Eddington ratio of 1.25 ± 0.19
 - ✧ Outflow velocity = $0.08c$ to $0.14c$ → extremely high velocity !!
- J0038–1527 is the first quasar found at the epoch of reionization with such strong outflows ! → These contribute the growth of the most massive galaxies !

Spectrum of J0038–1527

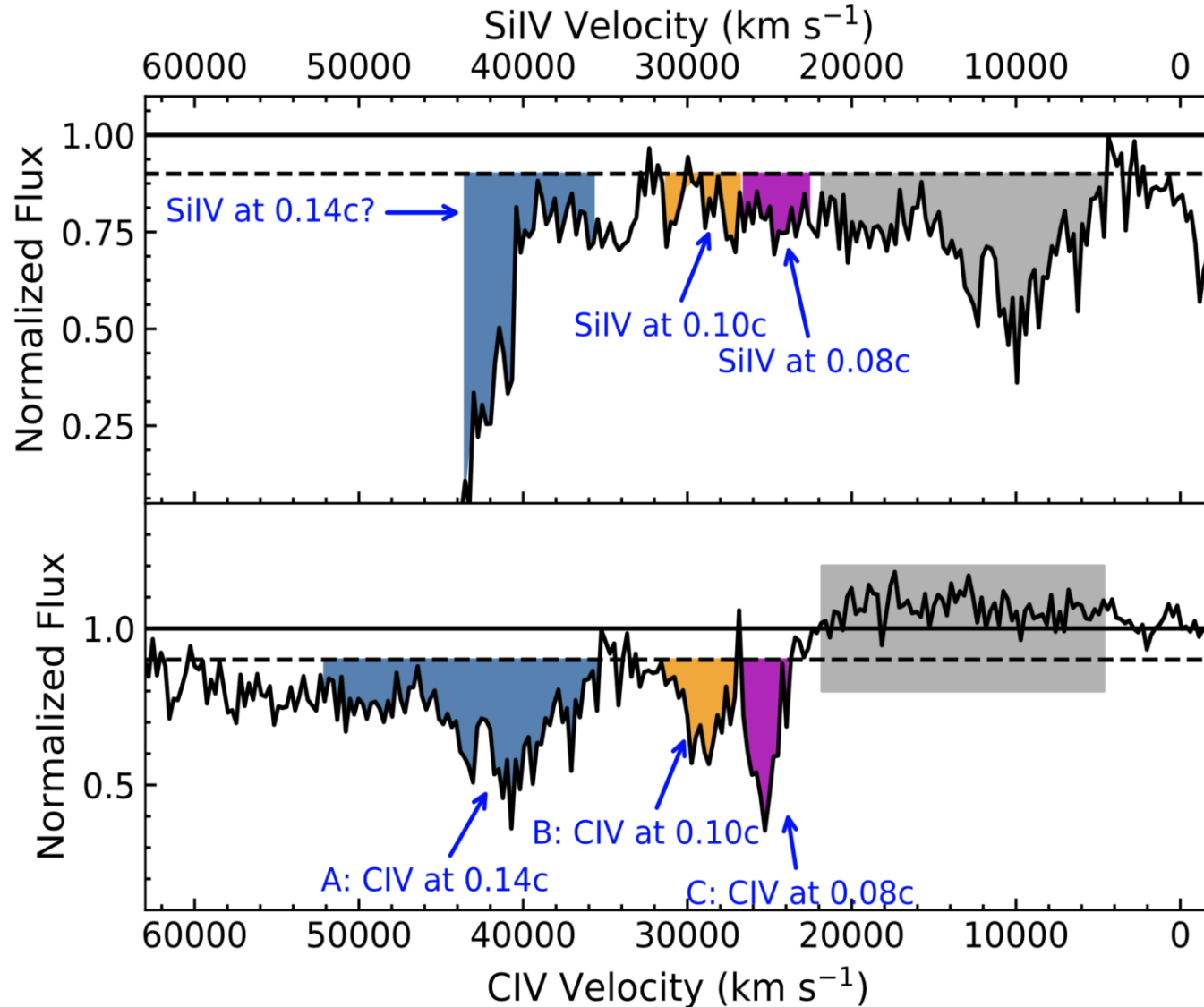


Gemini/GNIRS, with a total exposure time of 4.2 hours

GNIRS ©Gemini

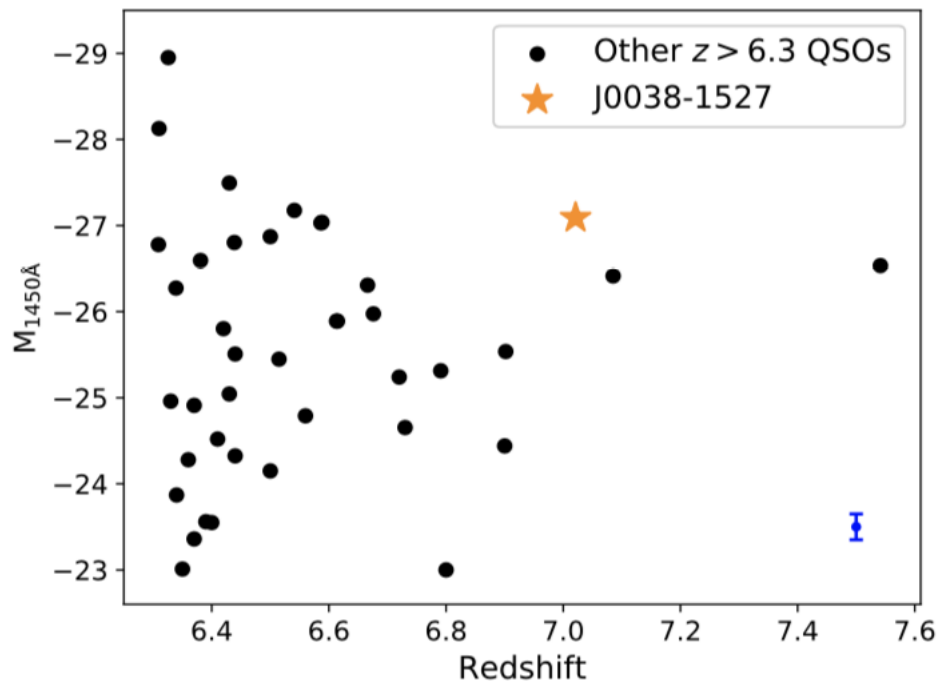


Normalized spectrum and BALs with extremely high velocity



- Normalized spectrum of J0038–1527
- The quasar has three absorption systems at **0.14c, 0.10c, and 0.08c** !
- BI = 3400 km/s (A), 890 km/s (B), 1010 km/s (C) for CIV BAL

Derived Parameters of J0038–1527



- J0038–1527 has high Eddington-ratio.

| | |
|--|-------------------------------|
| z_{MgII} | 7.025 ± 0.005 |
| z_{CIV} | 6.939 ± 0.008 |
| α_{λ} | -1.54 ± 0.05 |
| $\Delta v_{\text{CIV}} - v_{\text{MgII}} \text{ (km s}^{-1}\text{)}$ | 3400 ± 411 |
| $\text{FWHM}_{\text{MgII}} \text{ (km s}^{-1}\text{)}$ | 2994 ± 140 |
| $\text{EW}_{\text{MgII}} \text{ (\AA)}$ | 16.5 ± 1.0 |
| $\text{FWHM}_{\text{CIV}} \text{ (km s}^{-1}\text{)}$ | 8728 ± 452 |
| $\text{EW}_{\text{CIV}} \text{ (\AA)}$ | 18.1 ± 1.4 |
| $\lambda L_{3000\text{\AA}} \text{ (erg s}^{-1}\text{)}$ | 4.19×10^{46} |
| $L_{\text{Bol}} \text{ (erg s}^{-1}\text{)}$ | 2.16×10^{47} |
| $M_{\text{BH}} \text{ (M}_{\odot}\text{)}$ | $(1.33 \pm 0.25) \times 10^9$ |
| $L_{\text{Bol}}/L_{\text{Edd}}$ | 1.25 ± 0.19 |

Summary of the two studies

- Conclusion: X-ray and optical/UV observation

- (At least) The X-ray absorbing material moving out of the line-of-sight, leaving an X-ray unabsorbed non-BAL quasar.
- The UV absorber might have become more highly ionized (in a shielding-gas scenario) or also moved out of the line-of-sight (in a wind-clumping scenario).

Sameer et al. (2018)

- J0038–1527 is the most luminous quasar known at $z > 7$ ($L_{\text{Bol}} = 5.6 \times 10^{13} L_{\odot}$)

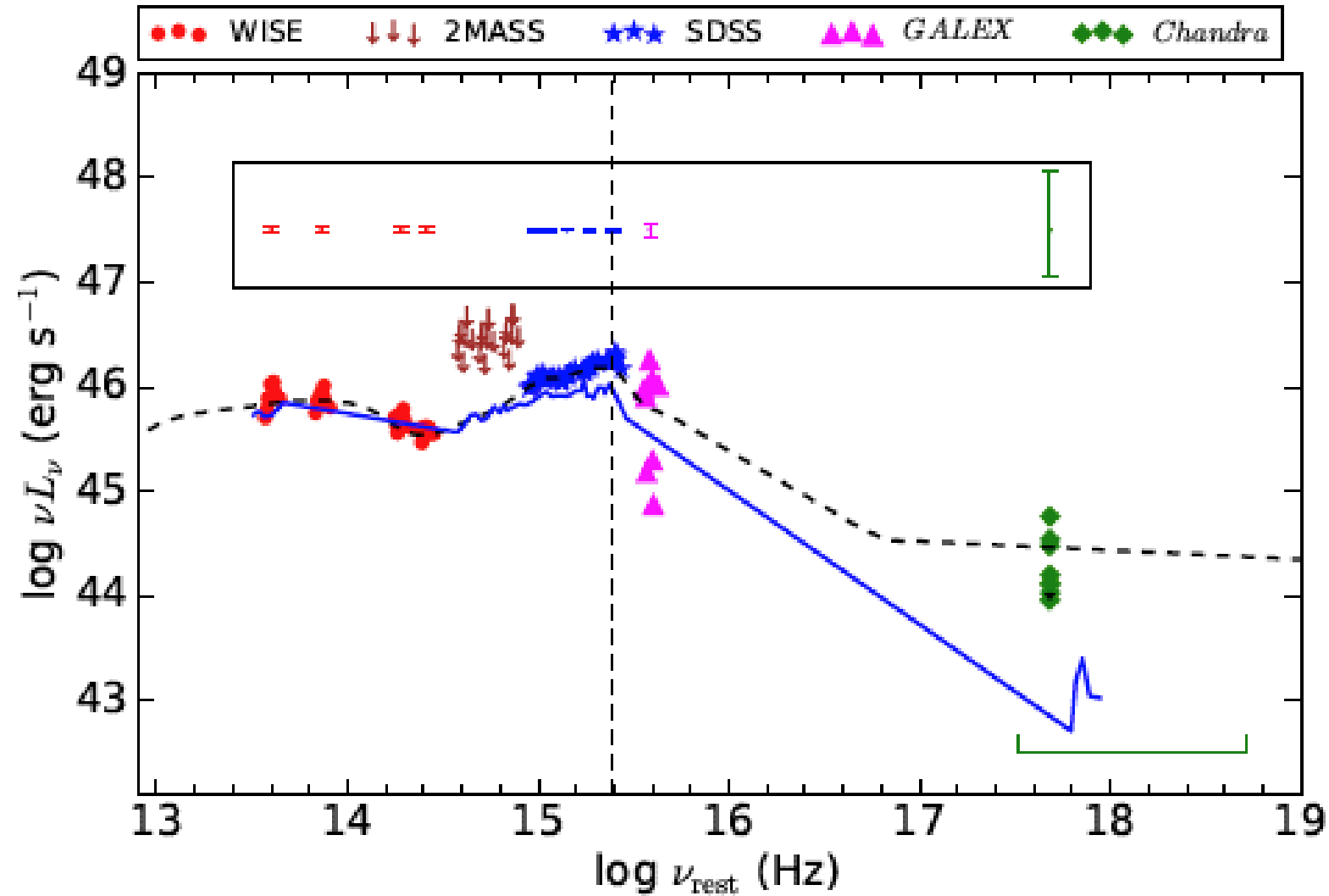
- ✧ Eddington ratio of 1.25 ± 0.19

- ✧ Outflow velocity = $0.08c$ to $0.14c$ → extremely high velocity !!

- J0038–1527 is the first quasar found at the epoch of reionization with such strong outflows ! → These contribute the growth of the most massive galaxies !

Wang et al. (2018)

Appendix I : SED (Samerr et al. 2018)



Appendix II : CIV Emission Blueshift (Wang et al. 2018)

